Microchemical Journal 129 (2016) 205–212

Contents lists available at ScienceDirect

Microchemical Journal

journal homepage: www.elsevier.com/locate/microc

Simultaneous determination of ascorbic and uric acids and dopamine in human serum samples using three-way calibration with data from square wave voltammetry

Adrian Marcelo Granero [a,1], Gastón Darío Pierini [a,1], Sebastián Noel Robledo [b,1], María Susana Di Nezio [c], Héctor Fernández [a,*], María Alicia Zon [a,*]

[a] Departamento de Química, Facultad de Ciencias Exactas, Físico-Químicas y Naturales, Universidad Nacional de Río Cuarto, Agencia Postal N°3, 5800 Río Cuarto, Argentina
[b] Departamento de Tecnología Química, Facultad de Ingeniería, Universidad Nacional de Río Cuarto, Agencia Postal N°3, 5800 Río Cuarto, Argentina
[c] Departamento de Química, INQUISUR, Universidad Nacional del Sur, B8999CPB, Bahía Blanca, Argentina

ARTICLE INFO

Article history:
Received 22 March 2016
Received in revised form 30 June 2016
Accepted 1 July 2016
Available online 2 July 2016

Keywords:
Ascorbic acid
Uric acid
Dopamine
Square wave voltammetry
Three-way calibration

ABSTRACT

We present for the first time a novel analytical method based on a model of three-way calibration using second-order data generated from the combination of records of forward (oxidation) and reverse (reduction) currents using a glassy carbon electrode modified with a dispersion of electrochemically reduced graphene oxide (GCE/RGO) as the working electrode, which can be obtained from a square wave voltammetry single experiment. This methodology was used for the simultaneous determination of ascorbic (AA) and uric (UA) acids, and dopamine (DO) in the presence de glucose (interfering species) in lyophilized human serum samples.
The serum samples have analyte different concentration levels (normal and pathological levels). The forward and reverse currents were pre-processed using AsLS and COW, to generate the second order data and finally the data were modeled with the U-PLS algorithm. Recovery studies were made in order to validate the proposed method. Recovery percentages between 92.4 and 120% were obtained.
The present method has the advantage to generate second order data through a simple voltammetric experiment. Among the advantages of the proposed method can be mentioned speed, easy data acquisition and the possibility of using modified electrodes with nano-structures.

1. Introduction

Ascorbic acid (AA) is an essential vitamin in the diet of humans and it is present in mammalian brain along with various neurotransmitter amines. It has been used in the prevention and treatment of the common cold, infertility, mental illnesses, cancers and respiratory viral infections [1,2].

Uric acid (UA; 7,9-dihydro-1H-purine-2,6,8-(3H)-trione) is the main final product of purine metabolism and, it is a very important substance for the human body. Abnormal levels of UA may be associated with many diseases, including Lesch–Nyhan syndrome, gout and hyperuricemia [3].

Dopamine (DO) is a neurotransmitter that plays an important role in central nervous system. Its determination is very important because of the necessity to monitor HIV infection, neurotransmission processes and diagnose Parkinson's disease [4,5].

AA, UA and DO usually coexist in biological matrixes. They are considered as crucial molecules for physiological processes in human metabolism [6]. Thus, the development of sensitive and selective detection methods for these bio-molecules is highly important in healthcare, biological analysis and clinical diagnostics.

Electrochemical techniques have received considerable interest for simultaneous detection of different analytes because of their high sensitivity, simple operation, rapid response and low cost. Potential pulses techniques are within electrochemical techniques mainly used for the development of analytical methods. The main advantage of the pulse voltammetric techniques is their ability to discriminate against charging currents. Thus, a higher sensitivity of the measured signal is achieved [7]. One of these pulse voltammetric techniques is called square wave voltammetry (SWV), which was invented by Ramaley and Krause [8]. In the last three decades, the advances in both analog and digital electronics allowed to SWV to be used in countless developments related to the quantification of various analytes [9–11].

* Corresponding authors.
E-mail addresses: agranero@exa.unrc.edu.ar (A.M. Granero), gpierini@exa.unrc.edu.ar (G.D. Pierini), srobledo@ing.unrc.edu.ar (S.N. Robledo), sdinezio@criba.edu.ar (M.S. Di Nezio), hfernandez@exa.unrc.edu.ar (H. Fernández), azon@exa.unrc.edu.ar (M.A. Zon).
[1] These authors contributed equally to this work.

http://dx.doi.org/10.1016/j.microc.2016.07.004
0026-265X/

As previously mentioned, AA, UA and DO are substances of great interest, so that the development of analytical methods for their simultaneous determinations is important in several areas such as science, health and clinical diagnosis.

However, the development of electrochemical methods is not easy because the oxidation peaks of AA, UA and DO exhibit overlapping at solid electrodes resulting in a poor selectivity [12]. Thus, several types of modified electrodes have been developed in recent years for the simultaneous determination of these analytes. Carbon based nanomaterials [13–15], noble metals [16,17], metal oxides [18,19], metal complexes [20] and polymers [21,22] have been used as effective electrode modifiers for the simultaneous determination of AA, UA and DO.

Recently, many materials based on graphene and its derivatives have been proposed to determine AA, UA and DO [23–25]. Reduced graphene oxide (RGO), a derivative of graphene, is usually obtained by chemical oxidation/exfoliation of graphite and subsequent reduction of graphene oxide (GO). Thermal, chemical and electrochemical reductions are among the usual methods of reducing GO to obtain RGO [26–30]. RGO has been successfully used for the simultaneous determination of AA, UA and DO in different real samples [31,32]. Chemometric tools are interesting complementary techniques, such as two or multiway analysis, that allow the simultaneous determination of several analytes having overlapping electrochemical signals or when there are strong interactions between these analytes or molecules present in the matrix analyzed [33,34].

Thus, several analytical methods have been developed by combining chemometric tools with electrochemical techniques for the determination of different analytes in complex matrices, using data of first and second order. For example, tocopherols were determined in edible vegetable oils [35], AA, UA, DO, and nitrite in human serum samples [36], flavonoids in pharmaceutical formulation [37], heavy metals in propolis [38], and ethiofencarb in the presence of interfering [39].

In this work, we discuss for the first time a novel analytical method based on a model of three-way calibration. It uses second-order data generated from the combination of records of forward (oxidation) and reverse (reduction) currents, which are obtained in the same experiment of square wave voltammetry. The proposed method is used for the simultaneous determination of AA, UA, and DO in lyophilized human serum samples.

2. Experimental and theoretical considerations

2.1. Experimental details

2.1.1. Reagents

AA, UA, DO, $KMnO_4$, H_2SO_4, Na_2HPO_4, NaH_2HPO_4, H_3PO_4, H_2O_2, and HCl, were purchased from Sigma–Aldrich. $HClO_4$, ethanol, methanol, and acetic acid were Merck p.a. Ultrapure water ($\rho = 18$ MΩ cm) was obtained from a Millipore-Milli Q system. Stock solutions of AA, UA and DO were prepared in ethanol, protected from light, and kept in the refrigerator. Working solutions were prepared daily by adding different aliquots of stock solutions to pH 7.00, 0.2 M phosphate buffer solution (PBS).

Graphene oxide (GO) was synthesized from graphite flakes by using a method developed by Marcano et al. [40].

2.1.2. Apparatus and software's

SW voltammetric experiments were performed with an Epsilon potentiostat (BASi—Bioanalytical System, USA) and run with the BAS Epsilon EC Windows software version 1.60.70. A C3 cell stand (BASi-Bioanalytical System, USA) was used for all experiments.

The electrodes were inserted into the cell through holes in its Teflon cover. The working electrodes were glassy carbon disks (GCE), GCE modified with a dispersion of GO (GCE/GO) and GCE modified with a dispersion of electrochemically reduced GO (GCE/RGO). A platinum wire and Ag/AgCl, 3 M NaCl (BAS, RE-5B) were used as counter and reference electrodes, respectively.

The MVC1 free algorithms package was employed to first order data analysis [41]. The MVC2 package was used to obtain second order models [41,42]. Artificial neural networks (ANN) were implemented from MATLAB 7.8 software.

2.1.3. Preparation of electrodes

Pretreatment of GCE: the electrodes were polished with alumina slurries of 0.30 and 0.05 μm for 1 min each, and sonicated in water during 30 s.

Preparation of GCE/GO: the polished GCE was modified with GO dispersion (GCE/GO) by dropping an aliquot of 5 μL of the dispersion on the top of the electrode and allowing to dry during 30 min at 37 °C.

Preparation of GCE/RGO: the GCE/RGO was electro-generated by applying at GCE/GO a potential of −1.70 V during 5 min in a pH 7.00 0.20 M PBS.

2.1.4. Procedure

The AA, UA and DO accumulation at the electrode surface was performed at open circuit potential during 5 min under stirring conditions. The voltammetric stripping was also performed in pH 7.00 0.20 M PBS.

SW voltammograms were recorded in the potential range from −0.4 to 0.8 V. Other parameters of SWV were: amplitude of the square wave, $\Delta E_{sw} = 0.025$ V, staircase potential, $\Delta E_s = 0.005$ V and frequency, $f = 20$ Hz.

2.2. Theoretical details

2.2.1. Generation of second-order data with SWV

Among several types of square wave voltammetry are of Osteryoung (OSWV) [43] and Barker (BSWV) [44]. However, the most frequently used is OSWV, which usually is called SWV.

SWV is a dynamic technique in which one pulse train is applied to the working electrode as shown in Fig. 1. Forward currents (I_f) are those currents measured at the end of direct pulses (in Fig. 1, m = 1, 3, 5, …). In contrast, reverse currents (I_r) are those measured in the same cycle in lower pulses (in Fig. 1, m = 2, 4, 6, …). The parameters of interest are ΔE_{sw}, ΔE_s, the period of the wave (τ), and the pulse time (t_p), defined as half of the period. The time parameter can also be described alternately by the frequency (f), where $f = \tau^{-1}$ or $f = 1/(2t_p)$ [45].

A very important aspect of SWV is that the forward and reverse currents can be examined independently of each other. The net current (I_n) is calculated as $I_f - I_r$ [43]. Forward and reverse currents have a diagnostic value and they are measured separately. Consequently, from a single SWV experiment it is possible to obtain three voltammograms, showing I_f, I_r, and I_n as a function of the potential (see Section 3.2.4.1). Thus, a SW

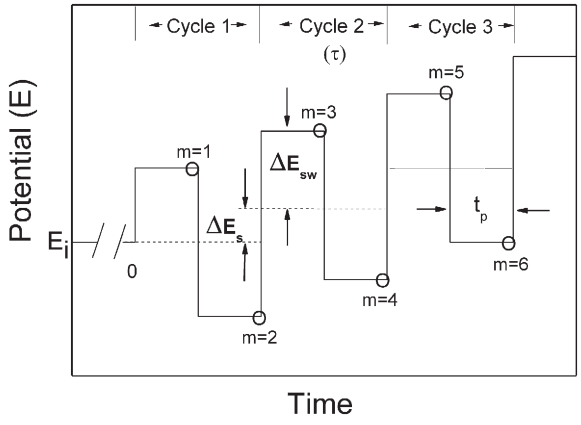

Fig. 1. Waveform and measurement scheme for square wave voltammetry.

voltammogram gives a data vector for I_f and another data vector for I_r, which can be array to generate second-order data. Thus, SWV is a very powerful tool because of it is possible to obtain first order data (net currents) or second order data (forward and reverse currents) without additional experimental cost.

2.2.2. First and second order calibration algorithms

Multivariate calibration (MVC) is a tool commonly used in many fields of chemistry, mainly in analytical chemistry. First order calibration has been widely used in electroanalytical techniques [36,38]. The algorithms commonly used are: partial least squares (PLS-1), multivariate curve resolution-alternating least squares (MCR-ALS), and artificial neural networks (ANN), and variations thereof. Previous algorithms can be classified in two classes: classical lineal (PLS-1, MCR-ALS) and nonlineal (ANN) [34]. These types of algorithms allow to model interactions between analytes and, also if it is known the presence of any interference and it is taken into account in the preparation of the calibration set, analyte/s can be modeled in the presence of interfering (first order advantage).

On the other hand, there are many algorithms available for processing multi-way data, based on few essential models. The choice of a particular model and algorithm should be primarily based on properties of the data [46].

An important property of second-order data is the trilinearity. A group of data matrices for a set of samples can in principle be arranged into a three-way data array. The array is considered to be trilinear if their elements can be reasonably fitted by the following expression (Eq. (1)):

$$x_{ijk} = \sum_{n=1}^{N} a_{in} b_{jn} c_{kn} + e_{ijk} \quad (1)$$

where a_{in} represents the relative concentration (also called score) of a given constituent n in the i-th sample, b_{jn} and c_{kn} are the intensities in both of the instrumental modes j and k, respectively (also called loadings), and e_{ijk} collects the fitting errors.

Algorithms based on the trilinear model are thus useful for multiway calibration from trilinear three-way data. One of the most employed trilinear algorithms is the parallel factor analysis (PARAFAC).

On the other hand, there are data that deviated from the trilinearity, which are intrinsically more complex than those of the type previously described. Thus, these data cannot yield trilinear three-way arrays, which requires models more flexible, such as non bilinear rank annihilation (NBRA) [47], and unfolded and multi-way partial least-squares (U-PLS and N-PLS) [48,49]. In the case of U-PLS, the calibration data matrix is unfolded, and PLS is applied using a suitable number of latent variables. This provides greater flexibility, being U-PLS more flexible than PARAFAC.

2.2.3. Pre-treatment of recorder data

In electrochemical measurements is common to observe changes in the baselines of the voltammograms and potential shifts in the discharge of each species studied. These events have been observed and reported previously in other works, which proposed different alternatives to solve these problems [36,38,50,51]. First, to solve the baseline problem, the algorithm Asymmetric Least Squares (AsLS) was employed in different voltammetric data such as SWV, and difference pulse voltammetry, DPV. This algorithm avoids the semi-manual and individual correction of baseline, which is subjective and time consuming [38]. For the shift in the potential discharge, two strategies have recently been used: *i*coshift [52] and correlation optimized warping (COW) [53]. Nascimento et al. used *i*coshift to solve the displacement in the discharge potential of six analytes in data obtained by adsorptive stripping voltammetry [54]. Other authors preferred to use the COW algorithm [36,38]. However, Jalalvand et al. [51] recently compared these two algorithms to resolve signals overlapping in DPV, and demonstrated that the COW algorithm generates the best results (in terms of errors of prediction) to correct the shift of the signal.

2.2.4. Model efficiency estimation

Model validation possibly is the most important step in the model building sequence. In order to evaluate the quality of quantitative predictions of concentrations obtained from the PLS-1, MCR-ALS, ANN and U-PLS models, the root mean square error (RMSE) between nominal and estimated concentrations for each analyte and relative errors of predictions (REP%) were calculated by applying Eqs. (2) and (3), respectively:

$$\mathrm{RMSE} = \sqrt{\frac{\sum_{i=1}^{n} (\hat{c}_i - c_i)^2}{n}} \quad (2)$$

$$\mathrm{REP}(\%) = \frac{100}{\bar{c}} \sqrt{\frac{\sum_{i=1}^{n} (\hat{c}_i - c_i)^2}{n}} \quad (3)$$

where $\hat{c}_i$ and c_i are estimated and nominal concentrations, respectively, and $\bar{c}$ is the average of nominal concentrations.

In addition, as the slope and the intercept are not statistically independent and there is always some degree of correlation between them, we analyzed if the point (1,0) was included in the elliptical joint confidence region (EJCR) of slope and intercept. Thus, we evaluated whether the concentrations estimated by PLS-1, MCR-ALS, ANN, and U-PLS models differ statistically from the nominal concentrations [55].

3. Results and discussion

3.1. Electrochemical behaviors of AA, UA and DO at different electrodes

The electrochemical behavior of AA, UA and DO in pH 7.00 0.2 M PBS was studied at different electrodes. Fig. 2 shows the net currents of square wave voltammograms recorded at bare GCE (blue line), GCE/GO (green line) and GCE/RGO (red line) for AA, UA and DO at a concentration of 1.0 mM.

These compounds show poorly defined signals and with a high degree of overlap between them at GCE or GCE/GO (blue and green lines, respectively in Fig. 2). On the other hand, well-defined peaks were found for the electro-oxidation of AA, UA and DO at GCE/RGO (red line in Fig. 2). These peaks show slightly higher currents than those found at GCE and GCE/GO, demonstrating an increase in the electroactive area due to the presence of RGO. In addition, a decrease in the oxidation potential of AA, UA and DO was found at GCE/RGO compared to those at GCE and GCE/GO. A likely explanation for this catalytic effect could be that these analytes

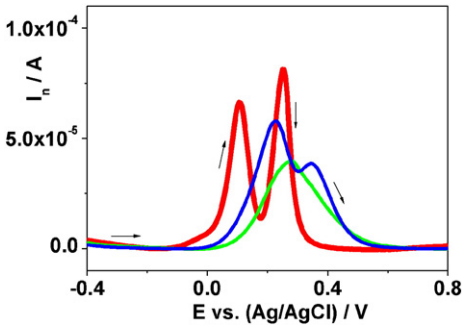

Fig. 2. SW voltammograms of AA, UA and DO recorded in PBS pH 7.00 0.2 M after an accumulation time of 5 min at open circuit potential at different electrodes: GCE (blue line), GCE/GO (green line) and GCE/RGO (red line). Analyte concentrations = 1 mM. ΔE_{sw} = 0.025 V, ΔE_s = 0.005 V and f = 20 Hz. Arrows indicate the direction of potential sweep.

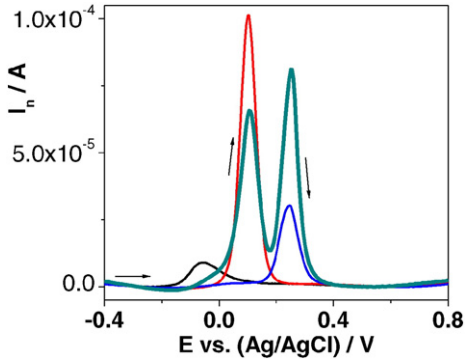

Fig. 3. SW voltammograms of AA (black line), UA (blue line) and DO (red line) and. a mixture of AA + UA + DO (dark cyan line). Other experimental conditions are the same that those in Fig. 2. Arrows indicate the direction of potential sweep.

present more favorable interactions with the GCE/RGO surface that with the other two surfaces. These results indicate that the CGE/RGO can be a good electrode material to develop electroanalytical methods to determine these substances in real samples.

3.2. Chemometric studies

3.2.1. Overlapping of electrochemical signals

Fig. 3 shows the net currents of square wave voltammograms recorded at GCE/RGO for every individual analyte and the mixture of them (AA, UA and DO). It is clear that the mixture of analytes produces a great overlapping of the signals, mainly that corresponding to AA (red line in Fig. 3). In addition, a strong interaction between the species adsorbed at the electrode surface is observed, which can be inferred from the change in the peak current magnitudes. This problem precludes the use of univariate calibration and promotes the use of multivariate calibration.

3.2.2. Calibration, validation and test sets

A calibration set was chosen according to a central composite design with the center point repeated on triplicated (16 experiments). These voltammograms were performed in pH 7.00 0.2 M PBS after an accumulation time of 5 min at an open circuit potential. A validation set of 12 mixtures was prepared in pH 7.00 0.2 M PBS with random concentrations in the ranges defined by the extremes of a central composite design. A test set of 9 experiments with random concentrations of AA, UA, DO and glucose (GLU) (which it is well known to be an interfering present in serum at high concentrations and is electrochemically oxidized in a potential region similar to that of the analytes) was prepared in the same buffer solution that the calibration and validation sets. To obtain the voltammograms corresponding to validation and test sets,

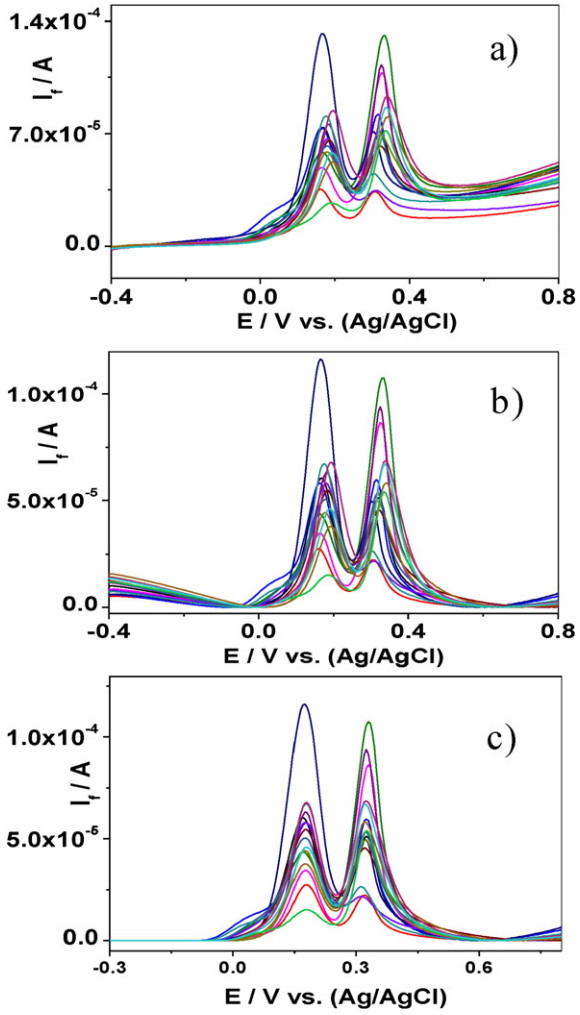

Fig. 4. a) Raw forward currents data related to calibration set, b) data corrected for baseline by AsLS related to calibration set and c) data corrected for shifts in the signals by COW related to calibration set.

Table 1
Concentrations of AA, UA and DO used in the calibration, validation and test sets.

Sample	Calibration (mM)			Sample	Validation (mM)			Sample	Test (mM)			
	AA	UA	DO		AA	UA	DO		AA	UA	DO	GLU
1	0.30	0.30	0.30	1	0.25	0.21	0.21	1	0.27	0.33	0.39	0.78
2	0.10	0.10	0.10	2	0.41	0.05	0.13	2	0.09	0.15	0.21	0.71
3	0.50	0.10	0.10	3	0.05	0.45	0.25	3	0.27	0.39	0.39	0.92
4	0.10	0.50	0.10	4	0.53	0.29	0.21	4	0.09	0.09	0.27	0.50
5	0.50	0.50	0.10	5	0.09	0.17	0.41	5	0.15	0.15	0.33	0.85
6	0.10	0.10	0.50	6	0.21	0.41	0.45	6	0.33	0.15	0.09	0.78
7	0.50	0.10	0.50	7	0.33	0.21	0.37	7	0.21	0.27	0.21	0.64
8	0.10	0.50	0.50	8	0.17	0.13	0.21	8	0.15	0.27	0.27	0.71
9	0.50	0.50	0.50	9	0.53	0.41	0.09	9	0.15	0.39	0.33	0.50
10	0.04	0.30	0.30	10	0.29	0.29	0.25	–	–	–	–	–
11	0.56	0.30	0.30	11	0.53	0.05	0.09	–	–	–	–	–
12	0.30	0.04	0.30	12	0.21	0.49	0.13	–	–	–	–	–
13	0.30	0.56	0.30	–	–	–	–	–	–	–	–	–
14	0.30	0.30	0.04	–	–	–	–	–	–	–	–	–
15	0.30	0.30	0.56	–	–	–	–	–	–	–	–	–
16	0.30	0.30	0.30	–	–	–	–					

Table 2
Values of root mean square errors and relative errors of predictions obtained by PLS-1, ANN, MCR and U-PLS for AA, UA and DO.

Analyte	Calibration approach	RMSEP (mM)	REP (%)	RMSEP (mM)	REP (%)
		Validation set		Test set	
AA	PLS-1	0.0631	21.0	0.1000	53.8
	ANN	0.1490	49.5	0.1020	54.8
	MCR	0.6405	213.5	0.4751	255.4
	U-PLS	0.0237	7.9	0.0308	16.0
UA	PLS-1	0.0787	26.2	0.0930	38.8
	ANN	0.1140	43.3	0.0900	37.5
	MCR	0.9166	348.1	0.5857	244.0
	U-PLS	0.0269	10.2	0.0266	11.8
DO	PLS-1	0.0928	30.9	0.12	41.7
	ANN	0.1224	53.2	0.1313	45.6
	MCR	1.265	542.1	1.218	422.8
	U-PLS	0.0240	9.1	0.0330	11.5

the experimental parameters were the same to the calibration set. The different concentrations of the calibration, validation and test sets are shown in Table 1.

3.2.3. Data preprocessing

In Section 2.2.3 we already explained the importance of process data obtained with the voltammetric techniques. For the baseline correction the AsLS algorithm was used. To correct the shift in the analytes discharge potential we use the algorithm COW. Fig. 4 shows a calibration set from raw forward currents data, baseline corrected data and, baseline-alignment data. These pretreatment was also employed for reverse and net currents.

3.2.4. Generation of the models

3.2.4.1. First order models. PLS-1, ANN, MCR-ALS were the first order algorithms used in this work. These algorithms are well known and there is much information in literature [56]. Thus, they will not be described here.

For the generation of PLS-1 models, the net currents versus potential pre-processed data with AsLS-COW were used. For the generation of ANN models, data used were those only corrected by the baseline. In addition, the MCR-ALS implementation was also made with only data corrected for the baseline. However, all first order models generated gave a poor prediction power, probably for the nature of the data (Table 2). Fig. 5a–d shows the net, forward and reverse currents obtained for the AA, UA, DO, and their mixture.

3.2.4.2. Second order model. U-PLS was the second order algorithm used in our work. This algorithm has already been described in detail [48]. The first step in the application of U-PLS was the assessment of the optimum number of calibration factors (A). This was done by resorting to the leave-one-out cross-validation procedure.

For the generation of U-PLS model, the data used were a result of a the cross product or vector product obtained from the forward and reverse currents after applying the data processing with AsLS and COW. Fig. 5e shows the second order data generated for the combination of both currents.

3.2.4.3. Comparison of predictive ability of the algorithms. In order for comparison of predictive ability of models, the predicted concentrations of both validation and test sets were compared on the nominal concentrations (results not shown). In this case an ordinary least squares (OLS) analysis of predicted concentrations versus nominal concentrations was applied [57]. The calculated values, intercept and slope were compared with their theoretically expected values, based on EJCR test. If the ellipses contain the values 0 and 1 for intercept and slope (ideal point), respectively, this fact demonstrates that the predicted and nominal values do not present significant difference at a 95% confidence level. Moreover, the elliptic size denotes precision of the analytical method; i.e., smaller size corresponds to higher precision [58]. Fig. 6 shows the corresponding ellipses obtained from EJCR analyses for PLS-1, ANN, and U-PLS. The ellipses for MCR-ALS were also calculated, but results achieved were less satisfactory than those obtained with the other algorithms previously mentioned (results not shown).

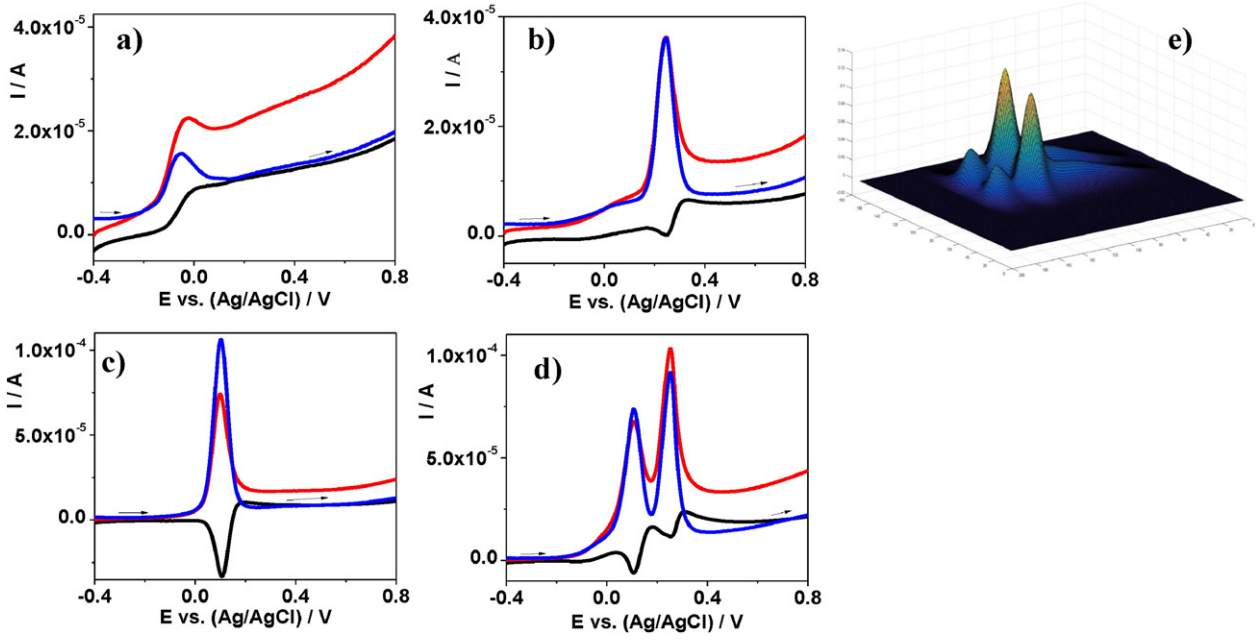

Fig. 5. Forward (red line), reverse (black line) and net currents (blue line) for (a) AA, UA (b), (c) DO and (d) the mixture of AA, UA and DO at the same experimental conditions as in Fig. 2. (e) Plot of second-order data.

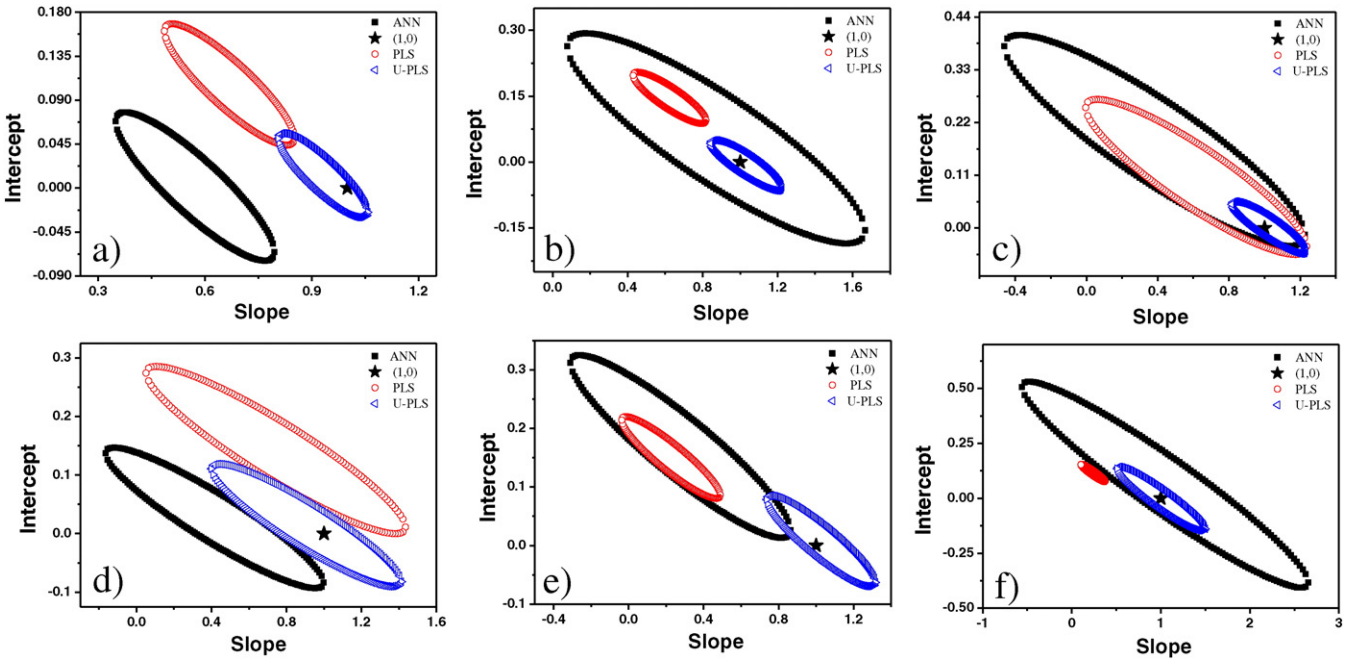

Fig. 6. Elliptical joint regions (at a 95% confidence level) of the validation set for (a) AA, (b) UA, (c) DO, and the test set (d) AA, (e) UA and (f) DO. In all cases the black star point indicates the theoretical (0,1) point. For both the validation and test sets, black, red and blue ellipses show ANN, PLS-1 and U-PLS results, respectively.

The RMSE and REP (%) obtained for all algorithms implemented are summarized in Table 2. The REP (%) found for U-PLS in the test set, are slightly higher than those of the validation set, due to the presence of unmolded interfering (GLU). Finally, it can be concluded that, based on the results of the ellipses and of RMSE and REP (%) values, the best predictions for AA, UA, and DO in both validation and test sets were obtained by U-PLS, which shows the accurate determination of analytes by the proposed methodology.

The fact of the best prediction of U-PLS can be due to the characteristics of the data under study, non-trilinearity of the three-way array and non-linearity between signals and concentrations.

3.3. Analysis of real samples

The developed analytical method was applied to determine AA, UA and DO in lyophilized human serum samples with different concentration levels (normal and pathological levels). Corrected forward and reverse currents (AsLS-COW) were used to generate the second order data and then implemented using the U-PLS model. Recovery studies were performed in order to validate the proposed method. Recovery percentages between 92.4 and 120% were obtained (Table 3).

Thus, this method has the advantage of generating second order data through one only experimental measurement. Among the advantages of the proposed method can be mentioned speed, easy data acquisition and the possibility of using modified electrodes with nano-structures.

4. Conclusions

We describe for the first time a novel and very interesting method analytical for the simultaneous determination of ascorbic and uric acids and dopamine in the presence de glucose (interfering species) in lyophilized human serum samples (normal and pathological levels). The developed method is based on a model of three-way calibration using second-order data generated from the combination of records of forward and reverse currents, obtained in the same square wave voltammetry experiment. In order to select the best model to predict the concentration of analytes, the predictive power of PLS-1, MCR-ALS, ANN and U-PLS through the analysis of the values of RMSE and REP and the analysis of ellipses. From these studies, it was concluded that the best results were obtained with U-PLS. The working electrode was a glassy carbon disk modified with reduced electrochemically graphene oxide.

Recovery studies were performed in order to validate the proposed method. Recovery percentages of the spiked samples varied between 92.4 and 120%, showing that the lyophilized human serum matrix does not show any significant interference in our analysis. The analytical

Table 3
Recovery studies. Results obtained for the simultaneous determination of AA, UA and DO in lyophilized human serum by using U-PLS.

Sample	AA			UA			DO		
	Added (mM)	Found (mM)	Recovery %	Added (mM)	Found (mM)	Recovery %	Added (mM)	Found (mM)	Recovery %
1	0.330	0.322	97.6	0.251	0.232	92.4	0.330	0.381	115
2	0.330	0.340	103	0.151	0.181	120	0.330	0.391	118
3	0.090	0.089	98.8	0.090	0.096	107	0.230	0.219	95.2
4	0.210	0.224	107	0.270	0.305	113	0.222	0.212	95.5
5	0.270	0.300	111	0.390	0.369	94.6	0.320	0.300	93.8

method proposed in this paper has two main advantages: 1) generating second order data through a single voltammetric experiment and, 2) speed, easy data acquisition and the possibility of using modified electrodes with nano-structures.

Acknowledgements

Financial support from Agencia Nacional de Promoción Científica y Tecnológica FONCYT (PICT 0916/2010), Consejo Nacional de Investigaciones Científicas y Técnicas (CONICET, PIP 112-201101-00184), Ministerio de Ciencia y Tecnología de la Provincia de Córdoba (MINCyT, PID 050/2010), and Secretaría de Ciencia y Técnica (SECyT) from Universidad Nacional de Río Cuarto (Res. Rec. 1230/2014) is gratefully acknowledged. G.D. Pierini thanks to CONICET for a postdoctoral fellowship.

References

[1] P.J. O'Connell, C. Gormally, M. Pravda, G.G. Guilbault, Development of an amperometric L-ascorbic acid (Vitamin C) sensor based on electropolymerised aniline for pharmaceutical and food analysis, Anal. Chim. Acta 431 (2001) 239–247.
[2] W.H. Sebrell, S. Harris (Eds.), second ed., The Vitamins, vol. 1, Academic Press, New York, 1967.
[3] F. Ni, Y. Wang, D. Zhang, F. Gao, M. Li, Electrochemical oxidation of epinephrine and uric acid at a layered double hydroxide film modified glassy carbon electrode and its application, Electroanalysis 22 (2010) 1130–1135.
[4] R.J. Marttila, in: W.C. Koller (Ed.), Handbook of Parkinson's Disease, Marcel Dekker, New York 1987, pp. 35–80.
[5] J.M. Savitt, V.L. Dawson, T.M. Dawson, Diagnosis and treatment of Parkinson disease: molecules to medicine, J. Clin. Invest. 116 (2006) 1744–1754.
[6] X.-B. Li, M. Rahman, G.-R. Xu, J.-J. Lee, Highly sensitive and selective detection of dopamine at poly(chromotrope 2B)-modified glassy carbon electrode in the presence of uric acid and ascorbic acid, Electrochim. Acta 173 (2015) 440–447.
[7] J.G. Osteryoung, J. O'Dea, in: A.J. Bard (Ed.), Electroanalytical Chemistry, Marcel Dekker, New York 1987, pp. 209–234.
[8] L. Ramaley, M.S. Krause Jr., Theory of square wave voltammetry, Anal. Chem. 41 (1969) 1362–1365.
[9] P.R. Perrotta, N.R. Vettorazzi, F.J. Arévalo, A.M. Granero, S.N. Chulze, M.A. Zon, H. Fernández, Electrochemical studies of ochratoxin mycotoxin at gold electrodes modified with cysteamine self-assembled monolayers. Its ultrasensitive quantification in red wine samples, Electroanalysis 23 (2011) 1585–1592.
[10] G.D. Pierini, A.M. Granero, M.S. Di Nezio, M.E. Centurión, M.A. Zon, H. Fernández, Development of an electroanalytical method for the determination of lead in Argentina raw propolis based on bismuth electrodes, Microchem. J. 106 (2013) 102–106.
[11] T. da Costa Oliveira, J. Machado Freitas, R.A. Abarza Munoz, E.M. Richter, A batch injection analysis system with square-wave voltammetric detection for fast and simultaneous determination of naphazoline and zinc, Talanta 152 (2016) 308–313.
[12] X. Ouyang, L. Luo, Y. Ding, B. Liu, D. Xu, A. Huang, Simultaneous determination of uric acid, dopamine and ascorbic acid based on poly(bromocresol green) modified glassy carbon electrode, J. Electroanal. Chem. 748 (2015) 1–7.
[13] Y.T. Shieh, H.F. Jiang, Graphene oxide-assisted dispersion of carbon nanotubes in sulfonated chitosan-modified electrode for selective detections of dopamine, uric acid, and ascorbic acid, J. Electroanal. Chem. 736 (2015) 132–138.
[14] J.Y. Sun, L.B. Li, X.P. Zhang, D. Liu, S.M. Lv, D.R. Zhu, T. Wu, T.Y. You, Simultaneous determination of ascorbic acid, dopamine and uric acid at a nitrogen-doped carbon nanofiber modified electrode, RSC Adv. 5 (2015) 11925–11932.
[15] H.L. Zou, B.L. Li, H.Q. Luo, N.B. Li, A novel electrochemical biosensor based on hemin functionalized graphene oxide sheets for simultaneous determination of ascorbic acid, dopamine and uric acid, Sensor Actuat. B-Chem. 207 (2015) 535–541.
[16] S. Ramakrishnan, K.R. Pradeep, A. Raghul, R. Senthilkumar, M. Rangarajan, N.K. Kothurkar, One-step synthesis of Pt-decorated graphene–carbon nanotubes for the electrochemical sensing of dopamine, uric acid and ascorbic acid, Anal. Methods 7 (2015) 779–786.
[17] S.Y. Wang, W. Zhang, X. Zhong, Y.Q. Chai, R. Yuan, Simultaneous determination of dopamine, ascorbic acid and uric acid using a multi-walled carbon nanotube and reduced graphene oxide hybrid functionalized by PAMAM and Au nanoparticles, Anal. Methods 7 (2015) 1471–1477.
[18] B. Kaur, B. Satpati, R. Srivastava, Synthesis of $NiCo_2O_4$/Nano-ZSM-5 nanocomposite material with enhanced electrochemical properties for the simultaneous determination of ascorbic acid, dopamine, uric acid and tryptophan, N. J. Chem. 39 (2015) 1115–1124.
[19] K. Ghanbari, N. Hajheidari, ZnO–CuxO/polypyrrolenanocomposite modified electrode for simultaneous determination of ascorbic acid, dopamine, and uric acid, Anal. Biochem. 473 (2015) 53–62.
[20] E.A. Khudaish, K.Y. Al-Ajmi, S.H. Al-Harthi, A solid-state sensor based on ruthenium (II) complex immobilized on polytyramine film for the simultaneous determination of dopamine, ascorbic acid and uric acid, Thin Solid Films 564 (2014) 390–396.
[21] R. Zhang, G.D. Jin, D. Chen, X.Y. Hu, Simultaneous electrochemical determination of dopamine, ascorbic acid and uric acid using poly(acid chrome blue K) modified glassy carbon electrode, Sensor Actuat. B-Chem. 138 (2009) 174–181.
[22] X.F. Liu, L. Zhang, S.P. Wei, S.H. Chen, X. Ou, Q.Y. Lu, Overoxidizedpolyimidazole/graphene oxide copolymer modified electrode for the simultaneous determination of ascorbic acid, dopamine, uric acid, guanine and adenine, Biosens. Bioelectron. 57 (2014) 232–238.
[23] A.A. Abdelwahab, Y.-B. Shim, Simultaneous determination of ascorbic acid, dopamine, uric acid and folic acid based on activated graphene/MWCNT nanocomposite loaded Au nanoclusters, Sensor Actuat. B-Chem. 221 (2015) 659–665.
[24] W. Cai, J. Lai, T. Lai, H. Xie, J. Ye, Controlled functionalization of flexible graphene fibers for the simultaneous determination of ascorbic acid, dopamine and uric acid, Sensor Actuat. B-Chem. 224 (2016) 225–232.
[25] X. Zhang, Y.-C. Zhang, L.-X. Ma, One-pot facile fabrication of graphene-zinc oxide composite and its enhanced sensitivity for simultaneous electrochemical detection of ascorbic acid, dopamine and uric acid, Sensor Actuat. B-Chem. 227 (2016) 488–496.
[26] S. Park, R.S. Ruoff, Chemical methods for the production of graphenes, Nat. Nanotechnol. 4 (2009) 217–224.
[27] S.F. Pei, H.M. Cheng, The reduction of graphene oxide, Carbon 50 (2012) 3210–3228.
[28] S.Y. Toh, K.S. Loh, S.K. Kamarudin, W.R.W. Daud, Graphene production via electrochemical reduction of graphene oxide: synthesis and characterization, Chem. Eng. J. 251 (2014) 422–434.
[29] C.K. Chua, M. Pumera, Chemical reduction of graphene oxide: a synthetic chemistry viewpoint, Chem. Soc. Rev. 43 (2014) 291–312.
[30] S.C. Ray, Application and uses of graphene oxide and reduced graphene oxide, Applications of Graphene and Graphene-Oxide Based Nanomaterials, William Andrew Publishing, Oxford 2015, pp. 39–55 (Chapter 2).
[31] L. Yang, D. Liu, J. Huang, T. You, Simultaneous determination of dopamine, ascorbic acid and uric acid at electrochemically reduced graphene oxide modified electrode, Sensors Actuators B Chem. 193 (2014) 166–172.
[32] Y.J. Yang, One-pot synthesis of reduced graphene oxide/zinc sulfide nanocomposite at room temperature for simultaneous determination of ascorbic acid, dopamine and uric acid, Sensors Actuators B Chem. 221 (2015) 750–759.
[33] Y. Ni, S. Kokot, Does chemometrics enhance the performance of electroanalysis? Anal. Chim. Acta 626 (2008) 130–146.
[34] N. Kumar, A. Bansal, G.S. Sarma, R.K. Rawal, Chemometrics tools used in analytical chemistry: an overview, Talanta 123 (2014) 186–199.
[35] S.N. Robledo, V.G.L. Zachetti, M.A. Zon, H. Fernández, Quantitative determination of tocopherols in edible vegetable oils using electrochemical ultra-microsensors combined with chemometric tools, Talanta 116 (2013) 964–971.
[36] M.B. Gholivand, A.R. Jalalvand, H.C. Goicoechea, T. Skov, Chemometrics-assisted simultaneous voltammetric determination of ascorbic acid, uric acid, dopamine and nitrite: application of non-bilinear voltammetric data for exploiting first-order advantage, Talanta 119 (2014) 553–563.
[37] A.Y. Tesio, S.N. Robledo, A.M. Granero, H. Fernández, M.A. Zon, Simultaneous electroanalytical determination of luteolin and rutin using artificial neural networks, Sensors Actuators B Chem. 203 (2014) 655–662.
[38] G.D. Pierini, M.F. Pistonesi, M.S. Di Nezio, M.E. Centurión, A pencil-lead bismuth film electrode and chemometric tools for simultaneous determination of heavy metals in propolis samples, Microchem. J. 125 (2016) 266–272.
[39] N.M. Díez, A.G. Cabanillas, A.S. Rodriguez, H.C. Goicoechea, Second-order advantage maintenance with voltammetric data modeling for quantitation of ethiofencarb in the presence of interferences, Talanta 132 (2015) 851–856.
[40] D.C. Marcano, D.V. Kosynkin, J.M. Berlín, A. Sinitskii, Z. Sun, A. Slesarev, L.B. Alemany, W. Lu, J.M. Tour, Improved synthesis of graphene oxide, ACS Nano 4 (2010) 4806–4814.
[41] A.C. Olivieri, H.C. Goicoechea, F.A. Iñón, MVC1: an integrated MatLab toolbox for first-order multivariate calibration, Chemometr. Intell. Lab. 73 (2008) 189–197.
[42] A.C. Olivieri, H. Wu, R. Yu, MVC2: a MATLAB graphical interface toolbox for second-order multivariate calibration, Chemometr. Intell. Lab. 96 (2009) 246–251.
[43] J.J. O'Dea, J. Osteryoung, R.A. Osteryoung, Theory of square-wave voltammetry for kinetic systems, Anal. Chem. 53 (1981) 695–701.
[44] J.G. Osteryoung, R.A. Osteryoung, Square wave voltammetry, Anal. Chem. 57 (1985) 101A–110A.
[45] V. Mirceski, S. Komorsky-Lovric, M. Lovric, in: F. Scholz (Ed.), Square-Wave Voltammmetry, Springer-Verlag, Berlin, 2007.
[46] G. Escandar, H. Goicoechea, A. Muñoz de la Peña, A. Olivieri, Second- and higher-order data generation and calibration: a tutorial, Anal. Chim. Acta 806 (2014) 8–26.
[47] B.E. Wilson, W. Lindberg, B.R. Kowalski, Multicomponent quantitative analysis using second-order nonbilinear data: theory and simulations, J. Am. Chem. Soc. 111 (1989) 3797–3804.
[48] S. Wold, P. Geladi, K. Esbensen, J. Øhman, Multi-way principal components-and PLS-analysis, J. Chemom. 1 (1987) 41–56.
[49] R. Bro, Multiway calibration. Multilinear PLS, J. Chemom. 10 (1996) 47–61.
[50] A.R. Jalalvand, M.B. Gholivand, H.C. Goicoechea, A. Rinnan, T. Skov, Advanced and tailored applications of an efficient electrochemical approach assisted by AsLSSR-COW-rPLS and finding ways to cope with challenges arising from the nature of voltammetric data, Chemometr. Intell. Lab. 146 (2015) 437.
[51] A.R. Jalalvand, M.B. Gholivand, H.C. Goicoechea, T. Skov, Generation of non-multilinear three-way voltammetric arrays by an electrochemically oxidized glassy carbon electrode as an efficient electronic device to achieving second-order advantage: challenges, and tailored applications, Talanta 134 (2015) 607.
[52] G. Tomasi, F. Savorani, S.B. Engelsen, Icoshift: an effective tool for the alignment of chromatographic data, J. Chromatogr. A 43 (2011) 7832–7840.
[53] P.H.C. Eilers, I.D. Currie, M. Durban, Comp. Stat. Data Anal 50 (2006) 61–76.
[54] D.S. Nascimento, M. Insausti, B.S.F. Band, S.G. Lemos, Simultaneous determination of Cu, Pb, Cd, Ni, Co and Zn in bioethanol fuel by adsorptive stripping voltammetry and multivariate linear regression, Fuel 137 (2014) 172–178.

[55] J. Riu, F.X. Rius, Assessing the accuracy of analytical methods using linear regression with errors in both axes, Anal. Chem. 68 (1996) 1851–1857.
[56] M. Esteban, C. Ariño, J.M. Diaz-Cruz, Chemometrics for the analysis of voltammetric data, Trends Anal. Chem. 25 (2006) 86–92.
[57] A.G. Gonzalez, M.A. Herrador, A.G. Asuero, Intra-laboratory testing of method accuracy from recovery assays, Talanta 48 (1999) 729–736.
[58] J.A. Arancibia, G.M. Escandar, Two different strategies for the fluorimetric determination of piroxicam in serum, Talanta 60 (2003) 1113–1121.